

**Universitat de Lleida**

Document downloaded from:

<http://hdl.handle.net/10459.1/63233>

The final publication is available at:

<https://doi.org/10.1016/j.scitotenv.2018.04.153>

Copyright

cc-by-nc-nd, (c) Elsevier, 2018



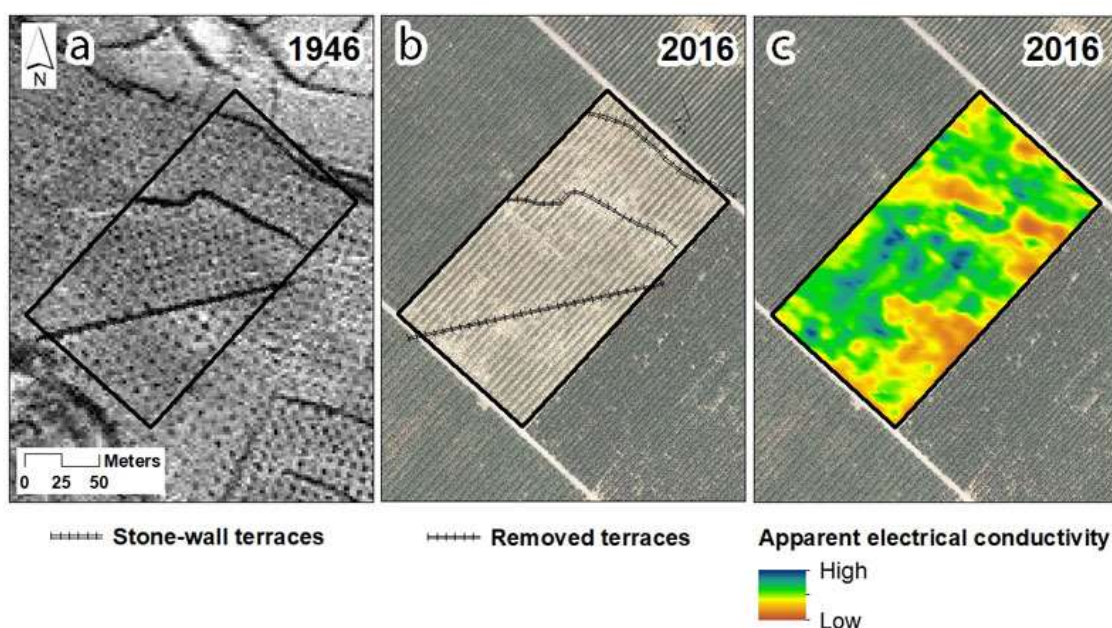
Està subjecte a una llicència de [Reconeixement-NoComercial-SenseObraDerivada 4.0 de Creative Commons](https://creativecommons.org/licenses/by-nc-nd/4.0/)

# Spatial variability in orchards after land transformation: consequences for precision agriculture practices

Asier Uribeetxebarria<sup>1\*</sup>, Elisa Daniele<sup>2</sup>, Alexandre Escolà<sup>1</sup>, Jaume Arnó<sup>1</sup> José A. Martínez-Casasnovas<sup>1</sup>

## Graphical abstract

Comparison of situations before (a) and after (b) land transformation, and (c) effects in the spatial variability of apparent electrical conductivity were stone-wall terraces were removed.



## Abstract

The change from traditional to a more mechanized and technical agriculture has involved, in many cases, land transformations. This has supposed alteration of landforms and soils, with significant consequences. The effects of induced soil variability and the subsequent implications in site-specific crop management have not been sufficiently studied. The present work investigated the application of a resistivity soil sensor (Veris 3100), to map the apparent electrical conductivity (ECa), and detailed multispectral airborne images to analyse soil and crop spatial variability to assist in site-specific orchard management. The study was carried out in a peach orchard (*Prunus persica* (L.) Stokes), in an area transformed in the 1980 decade to change from rainfed arable crops to irrigated orchards. A total of 40 soil samples at two depths (0-30 cm and 30-60 cm) were analysed and compared to ECa and the normalised difference vegetation index (NDVI). Two type of statistical analysis were performed between ECa or NDVI classes with soil properties: a linear correlation analysis and multivariate analysis of variance (MANOVA). This method was preferred instead of a separate analysis of variance (ANOVA) to avoid misleading and inconsistent results. The results showed that the land transformation could have altered the spatial distribution and continuity of soil properties. Although a relationship between ECa and peach tree vigour could be expected, it was not found, even in the case of trees planted in soils with salts content above the tolerance threshold. Two management zones delineation strategies were proposed: a) zones delineated according to the combined ECa classes, mainly addressed to leach salts in the high ECa zone, and b) zones delineated according NDVI classes to regulate tree vigour and yield. These strategies respond to the alteration of the original soil functions due to the land transformation carried out in previous years.

**Key words:** land use change, apparent electrical conductivity, vegetation index, potential management zones, MANOVA

## 1. Introduction

Since the mid-twentieth century, and particularly since the 1980s-90s, traditional agriculture is undergoing a change to a more modern, mechanized and technical agriculture. In many cases, these changes have involved land transformation, with land use alteration and intensification (Ritcher, 1984). This has been the case of cash crop development by the market-oriented agriculture. It is a global phenomenon that has promoted the expansion of hazelnut, rubber, fruit, and tea in developing tropical and subtropical countries (Xiao et al., 2015); citrus in Brazil (Moraes et al., 2017); or vineyards, almonds, olive and fruit trees in the Mediterranean Europe (García-Ruiz, 2010; Martínez-Casasnovas et al., 2010a), among others.

This intensification of agriculture has supposed the alteration of landforms and soils, with significant ecological consequences (Xiao et al., 2015). Some works have reported specific examples of those effects. For example, local hydrology (Yi et al., 2014), soil profile dismantlement (Laudicina, et al. 2016; Öztekin, 2013), acceleration of soil erosion (García-Ruiz, 2010; Ramos and Martínez-Casasnovas, 2010; Xiao et al., 2015), fragmentation of traditional landscapes (de Oliveira et al., 2017), increase of CO<sub>2</sub> emissions (Carlson et al., 2013), elimination of traditional soil conservation measures and increase of soil spatial variability (Laudicina et al., 2016; Martínez-Casasnovas and Ramos, 2009; Su et al., 2016; Xiao et al., 2015). Another major problem is the effect of topsoil removing on plant growth. Reduced growth may occur on the fill areas (Martínez-Casasnovas et al., 2010b), although the exposure of subsoil in the cuts is usually a more serious problem (Öztekin, 2013). Moreover, many of these land transformations have been supported by subsidies, as happens in the Mediterranean Europe, where many orchards planted in the last decades were also supported by the European Agricultural Policy in response to market demand (Cots-Folch et al., 2009; Nainggolan et al., 2012).

Although there have been attempts to document the process of cash crops expansion, the effects of induced soil variability due to land transformations and the subsequent implications in crop management have not been sufficiently investigated. However, this is of particular interest to fruit growers since, due to the soil-plant interaction, fruit trees development and their potential production are affected by the spatial variability of soil properties (Khan et al., 2016; Panda et al., 2010; Pedrera-Parrilla et al., 2016). Then, changes produced by land transformations can become a main constraint to consider when planning orchard management operations (Fulton et al., 2011). On the other hand, field size should not be considered as a limitation for precision agriculture applications in fruticulture since, even in small orchards, there may be differences in soil properties affecting tree growth and fruit quality (Käthner and Zude-Sasse, 2015; Zude-Sasse et al., 2016).

Soil information is often not available at a spatial resolution intrinsically needed for precision agriculture or other site-specific soil uses and management purposes (Mertens et al., 2008); and specifically is not available after land transformations. One approach to obtain detailed spatially distributed soil data is the non-invasive measurement of the apparent electrical conductivity (ECa). Soil sensors for on-the-go ECa mapping are increasingly used for this purpose (Corwin and Lesch, 2003; Fulton et al., 2011; Mertens et al., 2008), and to delineate management zones according to the concept of precision agriculture (Moral et al., 2010; Peralta and Costa, 2013). In orchards, ECa has been used for the analysis of soil variability, and some researchers have found correlations between ECa, generative tree growth, fruit development and fruit size (Käthner and Zude-Sasse, 2015; Zude-Sasse et al., 2016). In this respect, it was pointed out that fruit development and soil ECa were well correlated. However, quality parameters, although very variable, are spatially less stable and may be poorly related to the ECa as indicated Aggelopoulou et al. (2010) in apple tree plantations. Regarding the interpretation of the ECa signal, some authors have highlighted the difficulty to determine the soil properties that most affect the variability of ECa in a particular field (Uribeetxebarria et al., 2018). Because of that, they proposed the use of multivariate analysis of variance (MANOVA) to better interpret which soil properties are behind the variation of the electrical conductivity signal. This was particularly useful in orchards affected by previous parcelling (Uribeetxebarria et al., 2018).

Additionally, site-specific management zones (SSMZ) can also be delimited based on remote sensing data. In this respect, the most frequently used vegetation index is the Normalised Difference Vegetation Index (NDVI) (Rouse et al., 1974), which is feasible in low-chlorophyll fruits and canopy imaging. NDVI is correlated to plant vigour and has strong interaction with yield and sometimes quality parameters (Zude-Sasse et al., 2016). Different authors have used spectral indices to estimate orchard variables. For example, Peña-Barragán et al. (2004) developed a methodology to determine tree cover in olive groves using aerial images and different spectral indexes. González-Dugo et al. (2013), using high resolution airborne thermal imagery, assessed the heterogeneity in water status in commercial orchards (almond, apricot, peach, lemon and orange), as a prerequisite for precision irrigation management. Other authors (Noori and Panda, 2016) also studied the relationship between vegetation indexes (SAVI, NDVI and Vegetative Vigour Index) with field environmental data including soil and tree structure attributes in an olive orchard, suggesting that these relationships would help in Site Specific Crop Management (SSCM) of orchards. Other works used airborne hyperspectral imagery for predicting yield in citrus crops (Ye et al., 2009), or more specifically, to quantify fluorescence emission in a commercial citrus orchard as well (Zarco-Tejada et al., 2016). In the latter, the objective was to track photosynthesis at different phenological and stress stages throughout the season to suggest its operational use in precision agriculture.

Despite these findings and advances, there are not many examples of practical application of SSCM in commercial fruit orchards (Noori and Panda, 2016). However, emerging research knowledge in this field demonstrates clear advantages of precision agriculture tools in fruit production management. In this respect, different authors suggest the combination of ECa with spectral vegetation indices to help in the delineation of SSMZ (De Benedetto et al., 2013; Ortega-Blu and Molina-Roco, 2016; Panda et al., 2010). This approach allows identifying homogenous sub-field areas related to the intrinsic properties of soil and, above all, differentiated crop response. This is because ECa, by itself, may not be a good estimator of the most commonly measured soil properties and, under irrigation and fertigation conditions, the vegetation status may be more affected by water and nutrient management than by soil properties (De Benedetto et al., 2013).

ECa and/or spectral vegetation indices have been mainly applied in field crops and vineyard (Priori et al., 2013), but fewer studies refer to their use in fruit orchards, and even less in Mediterranean latitudes. One important reason could be the small sized orchards usually have there. Nevertheless, and as pointed out by Käthner and Zude-Sasse (2015) and Arnó et al. (2017), even in small orchards there may be differences in soil properties affecting tree growth and fruit quality.

As showed above, precision agriculture applications in tree crops are rather limited in the literature (Aggelopoulou et al., 2011). Moreover, as suggested by Öztekin (2013), after land transformations, some site-specific management practices should be taken into account to regain productivity and improve homogeneity in soil properties. However, to the best of our knowledge, there are no works addressing the implications of land transformations in precision agriculture. In this context, the present work investigated the application of detailed airborne images and a resistivity soil sensor to analyse soil and crop spatial variability to assist in site-specific orchard management. The study was carried out in a peach orchard (*Prunus persica* (L.) Stokes) located in Lleida (Catalonia, NE Spain). The area suffered land transformations in the 1980 decade to enlarge fields and changed from rainfed arable crops to irrigated orchards.

## 2. Materials and Methods

### 2.1. Study area

The research was carried out in a 2.24 ha commercial peach tree orchard located 20 km south from the city of Lleida (Catalonia, NE Spain) (Lat 41.477157°, Long 0.509500° WGS84) (Fig.1). It was planted in 2012 with white peach (*Prunus persica* (L.) Stokes, var. Patty), which is early harvested. The training system was the so-called "Catalan" vase or vessel shape, with a plantation pattern of 5x2 m. Peach trees were fertirrigated by means of a drip irrigation system. The system consisted of one irrigation sector, with one drip tubing per tree row and two emitters of 2 l h<sup>-1</sup> per tree. Three zone control valves were installed in the middle of the plot to turn on and off the water to the drip tubes by means of an irrigation controller/timer.

The elevation ranges from 156 – 167 m a.s.l. The slope is gentle to moderate, with an average of 5.3 % and a direction almost parallel to the tree rows (Fig. 1). The current morphology is the result of land clearing and levelling carried out during the 1980 decade. Previously, the relief was composed of low hills, with terraces protected with stone walls. Land transformation was carried out with heavy machinery (bulldozers). First, stones were removed from the old terraces and then terrain was smoothed. The upper more fertile soil layer was not specifically preserved. Marls and calcareous rocks belonging to the subsoil were put on the surface.

Soils of the area were classified as Typic Xerorthent, coarse-silty, mixed (calcareous), thermic (Soil Survey Staff, 2014). They have a typical sequence of horizons Ap-Bw-C (lutites), with the latter usually presenting a moderate salt content.

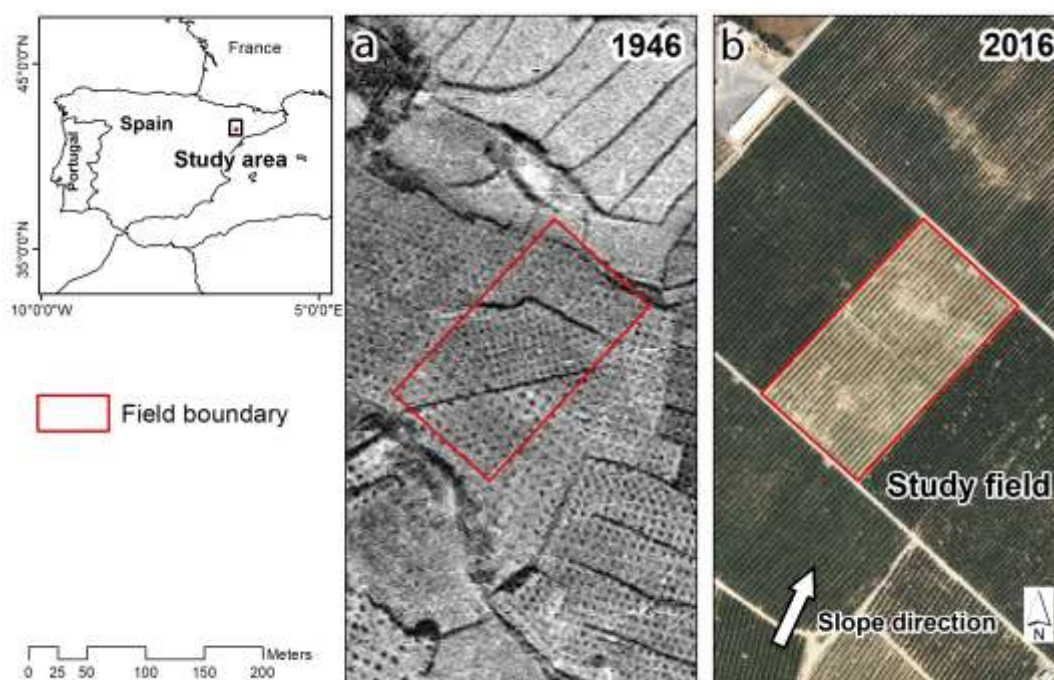


**Fig. 1.** Location of the study area and comparison of land uses and crop system before and after the land transformation carried in the 1980 decade. (a) Orthophoto of 1946 showing rainfed almonds, olive tree groves and winter cereals cultivated on terraces. (b) Orthophoto of 2016 showing modern peach orchards cultivated on larger plots without soil conservation terraces and under drip irrigation. (Orthophoto source: Cartographic and Geologic Institute of Catalonia).

## 2.2. Apparent electrical conductivity survey

An ECa survey was conducted on March 1st, 2016. The survey was carried out with a Veris 3100 sensor (Veris Technologies Inc. Salina, Kansas, USA). Veris 3100 uses two ECa arrays to measure the 0-30 cm (shallow ECa) and 0-90 cm (deep ECa) soil depths simultaneously. Data was georeferenced by means of a Trimble AgGPS332 receiver with EGNOS differential correction in geographic coordinates WGS84 (EPSG 4326). ECa values above or below  $\pm 2.5$  standard deviations (SD) were considered outliers and were removed from the original data file according to the criteria of Taylor et al. (2007). The final ECa data set consisted of 1668 points with shallow and deep readings. For interpretation and comparison purposes, ECa values were standardized at the reference temperature of 25 °C. In order to do that, a polynomial function was used as proposed by Sheets and Hendrickx (Ma et al., 2011). The adjusted ECa values were then renamed to EC<sub>25</sub> and expressed in dS m<sup>-1</sup> at 25 °C. These data were interpolated on a 1-m grid by means of ordinary kriging using the exponential semivariogram model. In addition, anisotropy was considered. This was because semivariance values presented a clear directional distribution in the NW to SE direction, perpendicular to the tree rows. For this purpose, ArcGIS Geostatistical Analyst 10.4 (ESRI, Redlands, California, USA) was used.



## 2.3. Soil sampling

Before soil sampling, an unsupervised classification of the shallow and deep EC<sub>25</sub> maps in 5 different classes was performed (Fig. 2) in order to stratify samples to obtain more structured information about the soil of the plot. For that, the ISODATA algorithm implemented in the Image Analyst of ArcGIS 10.4 was applied. The ISODATA is a *k*-means algorithm that uses minimum Euclidean distance to assign a cluster to each candidate pixel in an iterative process (Jensen, 1996), removing redundant clusters or clusters to which not enough pixels are assigned. Table 1 shows the average and standard deviation of the shallow and deep EC<sub>25</sub> in the 5 classes that showed increasing electrical conductivity values.

**Table 1.** Unsupervised classes based on the shallow and deep EC<sub>25</sub> and basic statistics (average and standard deviation) for each class.

Class	Shallow EC <sub>25</sub> dS m <sup>-1</sup> at 25 °C	Deep EC <sub>25</sub> dS m <sup>-1</sup> at 25 °C
1	0.74±0.20	0.69±0.18
2	1.21±0.18	1.02±0.17
3	1.57±0.15	1.32±0.16
4	1.93±0.14	1.58±0.17
5	2.39±0.19	1.86±0.19

In each EC<sub>25</sub> class, eight sampling points were randomly distributed, considering a minimum distance of 30 m between sampling points. This minimum distance corresponded to the range of the exponential semivariogram to interpolate ECa data from the Veris 3100 sensor. A total of 40 points were sampled in the plot (Fig. 2). Soils were sampled with an auger up to 90 cm or up to the limiting layer depth. This limiting layer corresponded to Tertiary lutites. The samples were taken in the space between the tree rows, between the central marks of the Veris 3100 coulter. The following properties were analysed for the 0-30 cm and 30-60 cm layers: pH, electrical conductivity 1:5 soil:water extract (EC<sub>1:5</sub>), equivalent calcium carbonate (CaCO<sub>3</sub>), cationic exchange capacity (CEC), particle-size (texture), water holding capacity (WHC) at -33 and -1500 kPa (field capacity and wilting point, respectively), and organic matter content (Org M) (the latter only at the 0-30 cm layer).

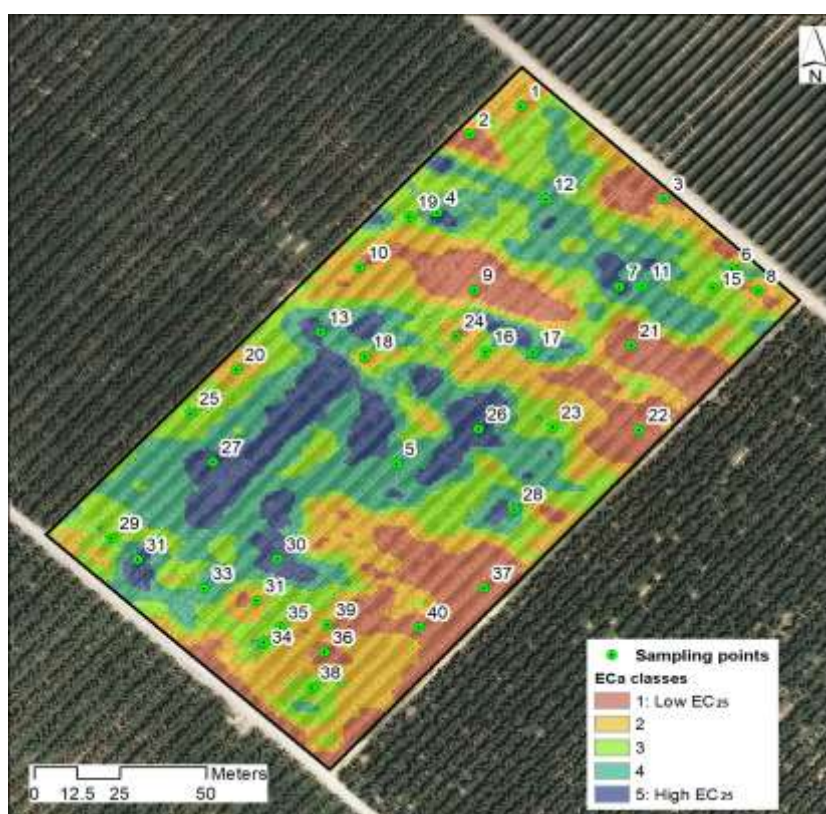


**Fig. 2.** Location of the soil sampling points stratified according to the spatial variability of EC<sub>25</sub> data organized in 5 classes. See Table 1 for class description.

## 2.4. Multispectral data acquisition and vegetation index

A 4-band multispectral image was acquired on May 16th, 2016 (approximately one month before harvest). For that, a Digital Multi-Spectral Camera (DMSC) (Specterra Services-Australia) mounted on a CESSNA 172S SKYHAWK airplane operated by RS Servicios de Teledetección (Lleida, Spain) was used. The DMSC captured four spectral bands 20 nm width, centred at 450 nm (blue), 550 nm (green), 675 nm (red) and 780 nm (near infrared). The spatial resolution of the image was 0.25 m. The image was pre-processed by the provider's software to compensate for miss-registration due to lens distortion, less than 0.2 pixels, and for scene brightness due to the bi-directional reflectance distribution function (Wallace et al., 2008). Absolute radiometric calibration was not carried out since the purpose of the study was not a multi-temporal analysis of the tree vigour.

The near infrared and red bands were used to calculate the Normalised Difference Vegetation Index (NDVI) (Rouse et al., 1974) according to Equation 1.

$$NDVI = \frac{NIR - Red}{NIR + Red} \quad (1)$$

where NIR is the near infrared band (780 nm) and Red the red band (675 nm) of the multispectral image.

Only the pixels including canopy vegetation of peach trees (NDVI > 0.4) were mapped (Fig. 3). These pixels were then used to define the tree canopy cover. This was done by converting the NDVI mask to a polygon layer and segmenting joined canopies into individual polygons. In this way, each tree in the plot was identified as an individual object. The polygons were used to calculate per tree NDVI zonal statistics (min, max, mean and standard deviation). These basic statistics were merged to the tree canopy layer. Finally, the polygons were converted to points using ArcGIS 10.4 and were stored in a point layer. The tool was forced to locate the

centroids inside the polygons (Fig. 3). With the trees represented by their centroids, ordinary kriging with an exponential semivariogram was performed to interpolate a surface with the NDVI-per-tree continuous spatial distribution.

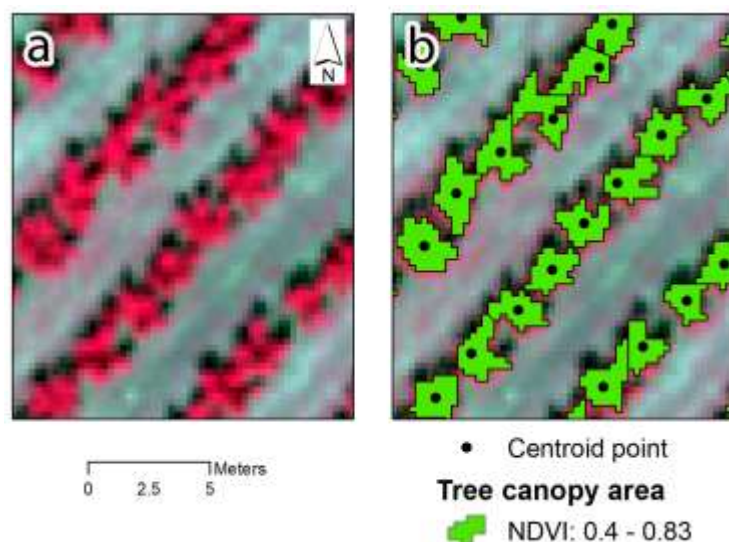


**Fig. 3.** (a) False colour composite RGB (NIR-Red-Green) of the airborne multispectral image acquired on May 16th, 2016 (pixel size 0.25 m). (b) Example of the tree canopy area derived from the classification of the NDVI above 0.4 and centroids of the tree canopy areas (polygons).

## 2.5. Statistical analysis

A linear correlation analysis (Pearson test) was carried out between individual soil properties,  $EC_{25}$  and NDVI values at the sampling points. As shown later, some unexpected differences were found in the relationships between the  $EC_{25}$  and NDVI with soil properties, probably because soil samples were taken in the alleys and not on the tree rows where localized irrigation can influence certain soil properties. For this reason, new 20 points situated upon the wet bulb and located 2.5 m from the previously sampling points were sampled and analysed (0-30 cm). To compare the means of the soil variables according to the location (inside or outside the wet bulb), a series of multiple  $t$ -tests were performed, adjusting the usual significance level of 0.05 with Bonferroni correction (Faraway, 2014). The software JMP Pro 12 (SAS Institute Inc.) was used for this purpose.

Different types of potential management zones were delineated according to the shallow and deep  $EC_{25}$  and NDVI surface data applying unsupervised classifications by means of the ISODATA algorithm implemented in the Image Analyst of ArcGIS 10.4. For each parameter, 2 classes (high and low values) were created. As proposed by Uribeetxebarria et al. (2018), the difference between high and low classes was determined by applying in each case a multivariate analysis of variance (MANOVA) of soil properties. This method was preferred instead of a separate analysis of variance (ANOVA) for each soil property to avoid misleading and inconsistent results. In fact,  $ECa$  and NDVI values can be considered as the result of the combined effect of soil properties as a whole (Corwin and Lesch, 2003), and delimitation of areas within the plot based on  $ECa$  or NDVI maps should be checked from a multivariate approach.

To interpret the results of the MANOVAs, a descriptive discriminant analysis (DDA) was used (Uribeetxebarria et al., 2018). As a result of the procedure, linear combinations of soil properties (discriminant functions) were provided, which managed to separate the two classes of  $EC_{25}$  (shallow or deep) or NDVI in a meaningful way. Standardized coefficients of each discriminant function (SDFCs) and structure coefficients (SCs) were used for interpretation. The first, SDFCs, were indicative of the contribution of each soil variable to the discriminant



function, whereas the SCs were the correlations between each observed variable and the discriminant function scores. The most important soil variables were finally identified through the parallel discriminant ratio coefficients (parallel DRCs), by multiplying SDFCs by the SCs. Then, parallel DRCs were used to identify non-redundant soil variables contributing to discriminate two types of soil in terms of EC<sub>25</sub> or NDVI.

### 3. Results

#### 3.1. Soil properties

The soils of the study area were characterised by a basic pH of 8.2±0.2 - 8.3±0.2 and an average EC<sub>1.5</sub> between 1.6±0.8 and 1.8±0.7 dS m<sup>-1</sup> at 25 °C (Table 2). In addition, soils had a high content of calcium carbonate (33.3±6.3 - 37.4±9.5 %). The average CEC was low to moderate (10.3±2.2 - 9.4±2.7 meq 100g<sup>-1</sup>). The organic matter content of the first layer was also low to moderate (2.2±0.7 %) and the AWHC of both layers was very similar (9.8±1.5 - 10.5±1.1%). Taking into account an average bulk density of 1400 kg m<sup>-3</sup>, the available water holding capacity (AWHC) in the average soil depth (61.1 cm) would be 86.8±11.1 mm, indicating a low AWHC for a xeric soil moisture regime and the necessity to irrigate the fruit trees. Regarding the texture, the most frequent textural classes were loam, clay loam or silty clay loam, which do not represent particular limitations for crop development.

**Table 2.** Basic statistics of soil properties for the 0-30 cm and 30-60 cm depth layers.

Soil property	0-30 cm	30-60 cm
pH <sub>1:2.5</sub>	8.2±0.2	8.3±0.2
EC <sub>1.5</sub> (dS m <sup>-1</sup> )	1.6±0.8	1.8±0.7
CaCO <sub>3</sub> (%)	33.3±6.3	37.4±9.5
CEC (meq 100g <sup>-1</sup> )	10.3±2.2	9.4±2.7
Org M (%)	2.2±0.7	-
WHC -33kPa (%)	22.7±2.8	23.2±2.4
WHC -1500kPa (%)	12.9±2.3	12.8±2.0
AWHC (%)	9.8±1.5	10.5±1.1
Clay (%)	23.9±5.8	25.6±4.6
Silt (%)	38.8±8.9	42.2±8.4
Sand (%)	34.8±10.6	30.7±12.1
Soil depth (cm) <sup>(1)</sup>	61.1±21.0	-

<sup>(1)</sup> The soil depth refers to the depth of the whole soil profile. The maximum measured soil depth was 90 cm, which was the maximum reached with the auger hole used for soil sampling.

#### 3.2. EC<sub>25</sub> and vegetation index: spatial pattern and comparison with former landforms

The soil volume explored by the Veris 3100 ECa surveyor presented average values of 1.54±0.52 dS m<sup>-1</sup> (0-30 cm) and 1.28±0.40 dS m<sup>-1</sup> (0-90 cm) at 25 °C.

As described in section 2.1 (study area), land levelling works were carried out prior to planting the fruit trees. Stone-wall terraces were removed in order to enlarge fields. Figure 4 shows the comparison between the location of the old stone-wall terraces and the apparent electrical conductivity surface (shallow and deep readings). Lower EC<sub>25</sub> values appeared in the northern part of the plot, where trees had also low vigour values, and in the southern part of the plot following the pattern of the terraces. Between the terraces there were higher EC<sub>25</sub> values, probably due to the existence of soils with higher clay content (23.4%) and less sand (34.7%) than in the southern part of the plot (21.7% clay and 43.5% sand), as result of the land levelling works.

Regarding NDVI, average per tree values ranged from 0.40 to 0.75. Two main zones could be distinguished: one with higher NDVI values, in the northern part of the plot, and another with lower NDVI values, in the south (Fig. 4).

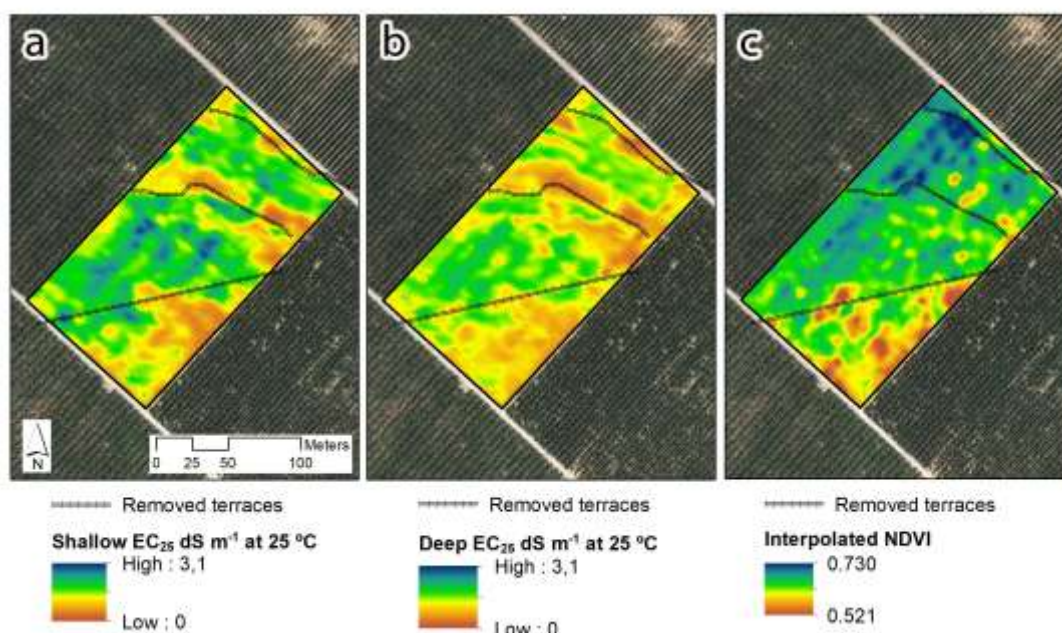


**Fig. 4.** Comparison between the locations of the removed stone-wall terraces, the apparent electrical conductivity ((a) shallow and (b) deep  $EC_{25}$   $dS\ m^{-1}$  at  $25\ ^\circ C$ ) and (c) the interpolated NDVI in the study plot.

### 3.3. Relationship between soil properties, $EC_{25}$ and vegetation index

Table 3 shows the correlation coefficients between the soil properties of the two analysed layers (0-30 cm and 30-60 cm), the  $EC_{25}$  (shallow and deep) and the NDVI. As expected, significant positive correlations were found between both measures of  $EC_{25}$  and  $EC_{1.5}$  (0.547 and 0.575,  $p$ -value  $< 0.01$ ). Regarding the availability of water, only the shallow  $EC_{25}$  showed a positive correlation with the WHC at -1500 kPa ( $p$ -value  $< 0.05$ ). On the other hand, soil depth presented a positive correlation ( $p$ -value  $< 0.01$ ) with both  $EC_{25}$  readings.

Differently from the relationships with the  $EC_{25}$ , the NDVI was not related to properties such as shallow or deep  $EC_{25}$ , nor with  $EC_{1.5}$ , water holding capacity or soil depth (Table 3). Only textural fractions coarser than clay were correlated. In the case of sand, the relationship was negative, probably indicating that at higher sand content the trees were less vigorous. This was an expected relationship since higher sand contents indicate less soil fertility. Regarding other properties, only the CEC at 30-60 cm showed a positive relationship with the NDVI. Although premature to conclude, this correlation would be expected as a sign of better soil fertility conditions in these locations.

To check the differences found before in the relationships between  $EC_{25}$  and NDVI with soil properties, Table 4 shows the results of the comparison of some soil properties ( $pH_{1.2.5}$ ,  $EC_{1.5}$ , organic matter and  $CaCO_3$ ) at 20 locations, inside and outside the wet bulb. The significant differences between samples inside and outside the bulb would explain the different expected relationship between soil properties and the  $EC_a$ , the latter measured outside the bulb; and between these same soil properties and the NDVI, the latter mainly conditioned by the drip irrigation system.

**Table 3.** Correlation coefficients between soil properties (0-30 cm and 30-60 cm), shallow and deep EC<sub>25</sub> and NDVI (N=40).

	Shallow EC <sub>25</sub> with 0-30 cm soil samples	Deep EC <sub>25</sub> with 30-60 cm soil samples	NDVI with 0-30 cm soil samples	NDVI with 30-60 cm soil samples
Shallow EC <sub>25</sub>	-	0.910**	0.002	-
Deep EC <sub>25</sub>	0.910**	-	0.156	-
pH <sub>1:2.5</sub>	-0.193	0.360*	0.110	-0.045
EC <sub>1:5</sub> (dS m <sup>-1</sup> )	0.547**	0.575**	0.075	0.164
CaCO <sub>3</sub> (%)	-0.086	0.037	0.119	0.062
CEC (meq 100g <sup>-1</sup> )	0.136	0.313	0.284	0.446**
Org M (%)	0.129	-	0.097	-
WHC -33kPa (%)	0.269	0.250	0.167	0.084
WHC -1500kPa (%)	0.337*	0.217	0.241	0.260
Clay (%)	0.207	0.252	0.048	0.253
Silt (%)	0.123	0.194	0.523**	0.194
Sand (%)	-0.197	-0.196	-0.365*	-0.233
Soil depth (cm)	0.439**	0.487**	0.077	-

\*p-value < 0.05; \*\* p-value < 0.01

**Table 4.** Comparison of some relevant soil properties inside and outside the wet bulb (0-30 cm). Results of t-test adjusted by the Bonferroni correction (N=20).

Soil property	Inside wet bulb	Outside wet bulb	t-test p-value
pH <sub>1:2.5</sub>	7.96±0.1	8.23±0.24	<0.01
EC <sub>1:5</sub> (dS m <sup>-1</sup> )	0.97±0.47	1.43±0.54	<0.01
Org M (%)	3.01±0.47	2.15±0.66	<0.01
CaCO <sub>3</sub> (%)	29.24±6.23	31.32±6.32	0.301

### 3.4. Zonal analysis between soil properties, EC<sub>25</sub> and vegetation index

In addition to the previous analysis, different multivariate analyses of variance (MANOVAs) were performed to determine specific soil properties mainly linked to the spatial variation of EC<sub>25</sub> and NDVI classes. Results are presented in Table 5. Regarding the shallow EC<sub>25</sub> classes, properties such as EC<sub>1:5</sub>, soil depth and clay were the ones that contributed most to the discriminant function explaining the spatial variation. The importance of those properties is highlighted by the parallel discriminant ratio coefficients (parallel DRC), which indicates the relative contribution of each soil property in the canonical function. Similarly, in the case of the deep EC<sub>25</sub> classes, the soil depth and EC<sub>1:5</sub> were also key properties in the variation of the ECa in addition to silt as a textural class. These results were similar to those obtained previously with the linear correlation analysis (Table 3). However, the use of MANOVAs made it possible to notice that, as expected, the use of ECa sensors is a good tool to indirectly observe the spatial variation of soil texture. On the other hand, the possible influence of the water content was now unnoticed. This should not be a major problem in the case of irrigation. From the point of view of land transformation, the ECa signal allowed to know the spatial variability of properties that are more stable in time, such as depth and soil texture, were now detected.

Regarding the NDVI classes, contribution to the discriminant function was found only for silt and sand contents in the top layer; and with the water holding capacity at -1500 kPa and silt content in the 30-60 cm layer (Table 5). The expected contribution of soil depth to differentiate NDVI classes was not found.

**Table 5.** Results of the descriptive discriminant analysis (DDA) of soil properties affecting EC<sub>25</sub> and NDVI at two different soil depths (0-30 cm and 30-60 cm).

		Soil properties (0-30 cm)										
		Depth	pH	EC <sub>1:5</sub>	CaCO <sub>3</sub>	Org M	CEC	Clay	Silt	Sand	WHC -33kPa	WHC -1500kPa
Shallow EC <sub>25</sub>	SDFC	0.64	-0.42	0.79	0.21	-	-0.16	0.86	-0.02	0.12	-	-0.24
	SC	0.51	-0.33	0.51	-0.11	-	0.133	0.32	0.13	-0.20	-	0.37
	Parallel DRC	0.33*	0.14	0.41*	-0.02	-	-0.02	0.28*	0.00	-0.03	-	-0.09
NDVI	SDFC	-0.18	-	0.10	0.37	0.32	-0.36	-	0.99	-0.26	-0.31	0.19
	SC	-0.02	-	0.03	0.21	0.36	0.57	-	0.86	-0.72	0.44	0.43
	Parallel DRC	0.00	-	0	0.08	0.12	-0.21	-	0.86*	0.19*	-0.13	0.08
		Soil properties (30-60 cm)										
		Depth	pH	EC <sub>1:5</sub>	CaCO <sub>3</sub>	Org M	CEC	Clay	Silt	Sand	WHC -33kPa	WHC -1500kPa
Deep EC <sub>25</sub>	SDFC	1.03	0.02	1.32	0.33	-	0.32	0.66	1.57	1.41	0.20	-1.30
	SC	0.48	0.22	0.33	-0.01	-	0.09	0.10	0.12	-0.11	0.09	0.07
	Parallel DRC	0.50*	0.00	0.44 *	0.00		0.03	0.07	0.19*	-0.16	0.02	-0.10
NDVI	SDFC	-	-0.87	0.54	0.74	-	-	-	1.29	1.52	-2.39	2.62
	SC	-	-0.16	0.14	0.16	-	-	-	0.13	-0.15	-0.04	0.23
	Parallel DRC	-	0.14	0.08	0.13	-	-	-	0.17*	-0.24	0.10	0.62*

SDFC: Standardized discriminant function coefficient; SC: structure coefficient; Parallel DRC: parallel discriminant ratio coefficient; Hyphens indicate variables that were removed to obtain significant discriminant functions. \* Indicates properties with a greater contribution to the discriminant function from MANOVA.

As previously noted, soil properties inside and outside the wet bulb vary significantly. Because of that, and although the spatial distribution of the EC<sub>a</sub> and the NDVI seem to follow similar patterns (Fig. 4), it is difficult to discern whether the NDVI varies linked to the variation of soil properties as a whole or, as the results of Table 5 seem to suggest, there is some local influence given the irrigation system used. In other words, it can be thought that there could be something altering the relationship between soil properties, EC<sub>25</sub> and NDVI. To find the reason of this alteration, a combination of the EC<sub>25</sub> and NDVI high and low classes was done and the coincidences and differences were mapped. The results can be observed in Fig. 5, which shows the four combinations of low and high EC<sub>25</sub> and NDVI classes, with the coincidences high-high and low-low showed in green colours. The major inconsistencies between NDVI and EC<sub>25</sub> were located upon the old terraces (in red and blue colours).



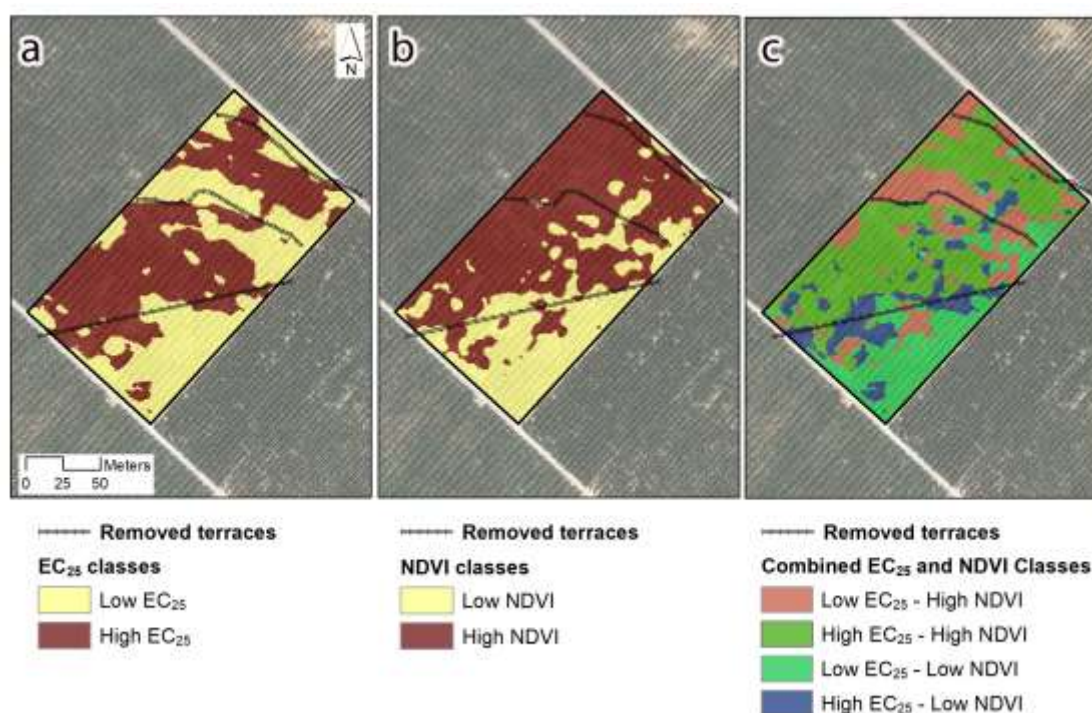


**Fig. 5.** Comparison between the location of old stone-wall terraces and (a)  $EC_{25}$  classes, (b) NDVI classes and (c) combined classes of  $EC_{25}$  and NDVI.

#### 4. Discussion

The soils of the study area were characterised by average  $EC_{1.5}$  values at 25 °C between  $1.6 \pm 0.8 \text{ dS m}^{-1}$  (0-30 cm) and  $1.8 \pm 0.7 \text{ dS m}^{-1}$  (30-60 cm) (Table 2), although there were maximum values of  $3.58 \text{ dS m}^{-1}$ . These mean values ( $< 2 \text{ dS m}^{-1}$  at 25 °C) were indicative of non-saline soils or slightly saline soils ( $2-4 \text{ dS m}^{-1}$  at 25 °C) (Rhoades et al., 1999). However, this classification refers to salinity in saturated extracts of soil, but not to the 1:5 extract analysed in this work. Therefore, this interpretation may not be conclusive, although induces to think that peach trees development could be influenced by salinity in some parts of the plot, since peach trees are sensitive to salts, with a threshold value around  $1.7 \text{ dS m}^{-1}$  at 25 °C. According to Tanji and Kielen (2002) and Stassen and Wooldridge (2011), yields begin to diminish at  $1.5 \text{ dS m}^{-1}$ , and at  $2.7 \text{ dS m}^{-1}$  yields may be reduced by 50% (Maas and Grattan, 1999 in Stassen and Wooldridge, 2011). The main effects of high salinity are reduction of water uptake and the onset of sodium and, particularly, chloride toxicities. These toxicities cause leaf burn, reduced vigour, stunted growth and low yields. Moreover, the slope of the reference regression line between electrical conductivity and yield is -21% (Tanji and Kielen, 2002), which indicates a fast yield decrease as salinity increases above the threshold.

Regarding the values of  $EC_{25}$  (shallow and deep), average values of  $1.54 \pm 0.52 \text{ dS m}^{-1}$  at 25 °C (0-30 cm) and  $1.28 \pm 0.40 \text{ dS m}^{-1}$  at 25 °C (0-90 cm), indicate that deep readings were lower on average, which is opposite to the  $EC_{1.5}$  measured in the soil samples. Nevertheless, both types of measures are not totally comparable, since deep measurements made with the ECa surveyor integrate the reading from 0 to 90 or 100 cm (Sudduth et al. 2005), and the results of the soil samples were specifically from 30 to 60 cm. The spatial pattern of both  $EC_{25}$  readings in Fig. 4 presents these differences in the average values, but shows the consistency and continuity of the signal in the two layers. However, the per tree NDVI pattern presented some relevant differences with respect  $EC_{25}$  variability. NDVI showed a more continuous and gradual distribution from the southern part of the plot to the northern part. Unlike the case of the  $EC_{25}$  spatial variability, the NDVI did not show a significant discontinuity where the old terraces were located (Fig. 4). This could reveal a specific behaviour of the fruit trees, in terms of

development, independent of the soil properties that determined the electrical conductivity readings by the resistivity sensor.

The analysis of the relationship between  $EC_{25}$  and NDVI (Table 3) revealed a lack of it. In addition, the results of the MANOVAs (Table 5) showed that the soil properties that contributed to the canonical discriminant functions of the  $EC_{25}$  and NDVI were not the same. In this case, the cause for this different behaviour between variables could be the influence of the fertigation system (drip irrigation), which maintains the root area free of salts, or with certain levels that are tolerated by the peach trees. This is in line with the findings of De Benedetto et al. (2013), who stated that under irrigation conditions vegetation might be more affected by water management than by soil properties. The results of Table 4 confirmed the hypothesis of the differences in relevant properties measured inside and outside the wet bulb, which could be responsible for the differences found in the relationships between the  $EC_{25}$  and the NDVI with soil properties. Except for the  $CaCO_3$  content, which was very high in both locations (inside and outside the bulb), the rest of the properties showed significant differences ( $p$ -value  $< 0.01$ ). It is worth noting the differences in the  $EC_{1.5}$ , which were significantly lower within the wet bulb. This means that peach trees were maintained with a tolerable salt content thanks to the drip irrigation system. In other words, tree vigour would not be affected by the salts content detected outside the wet bulbs by the  $ECa$  surveyor. The same reasoning could be applied to the lack of relationship between NDVI and soil depth. One could expect the higher the soil depth, the higher vigour trees, but this was not the case in the present study orchard, because the water and nutrients were supplied by fertigation and soil depth ( $61.1 \pm 21.0$  cm) is not a constraint for tree development.

As mentioned above, the lack of relationship between  $EC_{25}$  and NDVI would be particularly affecting the areas where differences in  $EC_{25}$  and NDVI classes occur (high-low and low-high), which were found where the old terraces were located in the past, before land transformation (Fig. 5). The removal of the terraces and the levelling influenced the  $ECa$ , since subsoil original materials (Tertiary marls with a variable content of salts) were put on the top layer, breaking the continuity of the original soils. This is what occurred in zones with high  $EC_{25}$  and low NDVI (Fig. 5 and Fig. 6). However, in the low  $EC_{25}$  and high NDVI zones the subsoil material put on surface were calcareous gravels, which provide better drainage conditions than the marls and lower salts content. In these zones, the local supply of water and fertilizers through the drip irrigation system would be providing the conditions for high tree vigour. Nevertheless, it could influence that there was not a good correspondence of  $EC_{25}$  and NDVI zones, as shown in the results.



**Fig. 6.** Saline patch in the high  $EC_{25}$  – low NDVI zone. In this area, Tertiary marls with variable salts content outcrop after the land transformation carried out to enlarge the field.

As regards the relationship between the soil properties and  $EC_{25}$  as derived from the readings of the Veris 3100 ECa surveyor, the MANOVA offers an added value with respect to either the linear relationship or the ANOVA (Uribeetxebarria et al., 2018). A separate analysis of each sampled soil property with respect to  $EC_{25}$  or  $EC_{25}$  classes (ANOVA) may lead to misleading and inconsistent results. In fact, ECa reflects the combined effect of soil properties as a whole, and the delimitation of areas within the plot based on ECa maps should be checked from a multivariate approach. In the present case, the results of the MANOVA are in line with the theoretical basis for the relationship between ECa and soil properties developed by Rhoades et al. (1999). The parallel DRC values of the discriminant functions for the shallow and deep  $EC_{25}$  (Table 5) show the contribution of  $EC_{1.5}$ , indicating that soil salinity is governing a significant part of the ECa readings. In addition, soil depth, clay and silt contents are also significantly contributing properties, in agreement with results reported in previous studies (Sudduth et al. 2005, Pedrera-Parrilla et al. 2016). In this case, the MANOVA was fundamental to identify clay as a relevant contributing property to the measured ECa, in comparison to the simple linear correlation analysis, in which clay was not correlated to  $EC_{25}$ . On the other hand, discriminant functions for the NDVI showed that textural classes silt and sand were behind the variation of the NDVI in the top layer, while the WHC at -1500kPa and silt did the same in the second layer.

The results confirmed the different behaviour of both types of variables ( $EC_{25}$  and NDVI) and suggest several possibilities of differential management in the orchard. In this respect, and although different authors have suggested the combination of ECa with spectral vegetation indices to help in the delineation of SSMZ (Panda et al, 2010; De Benedetto et al., 2013; Ortega-Blu and Molina-Roco, 2016), in the present case, and because of the lack of relationship between  $EC_{25}$  and NDVI, we propose two strategies. One of them would be delineating SSMZ according to the combined  $EC_{25}$  classes, which would mainly serve to increase the irrigation doses in the high  $EC_{25}$  zones to reduce the salts content in the root zone and to enlarge the dimensions of the wet bulb. At present, this recommendation would not be easy to implement because the irrigation system consists of only one sector, since it was designed without having into account the soil spatial variability. Nevertheless, it would be possible to actuate by increasing the number of emitters per tree in those zones of high  $EC_{25}$  zones.

The second strategy would be delineating SSMZ according to NDVI classes, which would serve as a reference to regulate the tree vigour and yield through different managements actions such as pruning, application of growth regulators or fruit thinning.

## 5. Conclusions

The present work is a contribution to the application of precision agriculture (PA) techniques in fruticulture (precision fruticulture, PF), which are not so extensively used as in arable crops. Specifically, PA and PF can help in establishing optimized management actions in those orchards where land transformations have occurred.

The results of soil sampling and ECa survey showed that land transformation carried out in the 1980 decade to enlarge fields could have altered the spatial distribution and continuity of soil properties. In this respect, although a relationship between apparent electrical conductivity and peach tree vigour could be expected, it was not found, even in the case of trees planted in soils with salts content above the tolerance threshold. This could be due to the drip irrigation system used in the orchard, which keeps the trees free of high salt contents in the root-explored region.

Adopting PA and PF strategies may be appropriate to manage the orchard according to SSMZ. In the present case, two management zones delineation strategies were proposed depending on the final objective of the action: a) zones delineated according to the combined  $EC_{25}$  classes, mainly addressed to leach salts in the high  $EC_{25}$  zone, and b) zones delineated according NDVI classes to regulate tree vigour and yield. These strategies respond to the alteration of the original soil functions due to the land transformation carried out in previous years.

**Acknowledgments:** This work was funded by the Spanish Ministry of Economy and Competitiveness through the AgVANCE Project (AGL2013-48297-C2-2-R). We are also grateful to Frutas Hermanos Espax SL for the possibility to carry out the research in its farm.

## References

Aggelopoulou, K., Wulfsohn, D., Fountas, S., Nanos, G., Gemtos, T., Blackmore, S., 2010. Spatial variability of yield and quality in an apple orchard. *Precis. Agric.* 11, 538–556. DOI 10.1007/s11119-009-9146-9

Aggelopoulou, K., Fountas, S., Pateras, D., Nanos, G., Gemtos, T., 2011. Soil spatial variability and site-specific fertilization maps in an apple orchard. *Precis. Agric.* 12, 118–129. <https://doi.org/10.1007/s11119-010-9161-x>

Arnó, J., Martínez-Casasnovas, J.A., Uribeetxebarria, A., Escolà, A., Rosell-Polo, J.R., 2017. Comparing efficiency of different sampling schemes to estimate yield and quality parameters in fruit orchards. *Advances in Animal Biosciences: Precision Agriculture (ECPA)*. 8:2, 471–476. <https://doi.org/10.1017/S2040470017000978>

Carlson, K.M., Curran, L.M., Asner, G.P., Pittman, A.M., Trigg, S.N., Adeney, J.M., 2013. Carbon emissions from forest conversion by Kalimantan oil palm plantations. *Nat. Clim. Change* 3, 283–287. <https://doi.org/10.1038/nclimate1702>

Corwin, D.L., Lesch, S.M., 2003. Application of Soil Electrical Conductivity to Precision Agriculture: Theory, Principles, and Guidelines. *Agron. J.* 95, 455–471.

Cots-Folch, R., Martínez-Casasnovas, J.A., Ramos, M.C., 2009. Agricultural trajectories in a mediterranean mountain region (Priorat, Ne Spain) as a consequence of vineyard conversion plans. *Land Degrad. Dev.* 20, 1-13. <https://doi.org/10.1002/ldr.856>

De Benedetto, D., Castrignano, A., Diacono, M., Rinaldi, M., Ruggieri, S., Tamborrino, R., 2013. Field partition by proximal and remote sensing data fusion. *Biosyst. Eng.* 114, 372–383. <https://doi.org/10.1016/j.biosystemseng.2012.12.001>

De Oliveira, S.N., De Carvalho Júnior, O.A., Gomes, R.A.T., Guimarães, R.F., McManus, C.M., 2017. Landscape-fragmentation change due to recent agricultural expansion in the Brazilian Savanna, Western Bahia, Brazil. *Reg. Environ. Change* 17, 411-423. <https://doi.org/10.1007/s10113-016-0960-0>

Faraway, J.J., 2014. Linear models with R. 2nd edition. London: Chapman and Hall/CRC, 286 pages.

Fulton, A., Schwankl, L., Lynn, K., Lampinen, B., Edstrom, J., Prichard, T., 2011. Using EM and VERIS technology to assess land suitability for orchard and vineyard development. *Irrigation Sci.* 29, 497-512. <https://doi.org/10.1007/s00271-010-0253-1>

García-Ruiz, J.M., 2010. The effects of land uses on soil erosion in Spain: A review. *Catena* 81, 1-11. <https://doi.org/10.1016/j.catena.2010.01.001>

González-Dugo, M.V., Zarco-Tejada, P.J., Nicolás, E., Nortes, P.A., Alarcón, J.J., Intrigliolo, D.S., Fereres, E., 2013. Using high resolution UAV thermal imagery to assess the variability in the water status of five fruit tree species within a commercial orchard. *Precis. Agric.* 14, 660–678. <https://doi.org/10.1007/s11119-013-9322-9>

Jensen, J.R., 1996. Introductory digital image processing: remote sensing perspective, 2nd ed., Prentice-Hall: Englewood Cliffs, NJ, USA.

Käthner, J., Zude-Sasse, M., 2015. Interaction of 3D soil electrical conductivity and generative growth in *Prunus domestica* L. *Eur. J. Hortic. Sci.* 80, 231–239. <https://doi.org/10.17660/eJHS.2015/80.5.5>



POSTPRINT of the article: Uribeetxebarria, A., Daniele, E., Escolà, A., Arnó, J., Martínez-Casasnovas, J.A. 2018. Spatial variability in orchards after land transformation: Consequences for precision agriculture practices. *Sci. Total Environ.* 635, 343-352. <https://doi.org/10.1016/j.scitotenv.2018.04.153>

Khan, F.S., Zaman, Q.U., Chang, Y.K., Farooque, A.A., Schumann, A.W., Madani, A., 2016. Estimation of the root zone depth above a gravel layer (in wild blueberry fields) using electromagnetic induction method. *Precis. Agric.* 17, 155-167. <https://doi.org/10.1007/s11119-015-9413-x>

Laudicina, V.A., Palazzolo, E., Piotrowska-Długosz, A., Badalucco, L., 2016. Soil profile dismantlement by land levelling and deep tillage damages soil functioning but not quality. *Appl. Soil. Ecol.* 107, 298-306. <https://doi.org/10.1016/j.apsoil.2016.07.002>

Ma, R., McBratney, A., Whelan, B., Minasny, B., Short, M., 2011. Comparing temperature correction models for soil electrical conductivity measurement. *Precis. Agric.* 12, 55-66. <https://doi.org/10.1007/s11119-009-9156-7>

Martínez-Casasnovas, J.A., Ramos, M.C., 2009. Soil alteration due to erosion, ploughing and levelling of vineyards in north east Spain. *Soil Use Manage.* 25, 183-192. <https://doi.org/10.1111/j.1475-2743.2009.00215.x>

Martínez-Casasnovas, J.A., Ramos, M.C., Cost-Folch, R., 2010a. Influence of the EU CAP on terrain morphology and vineyard cultivation in the Priorat region of NE Spain. *Land Use Policy* 27, 11-21, <https://doi.org/10.1016/j.landusepol.2008.01.009>

Martínez-Casasnovas, J.A., Ramos, M.C., Espinal-Utgés, S., 2010b. Hillslope terracing effects on the spatial variability of plant development as assessed by NDVI in vineyards of the Priorat region (NE Spain). *Environ. Monit. Assess.* 163, 379-396. <https://doi.org/10.1007/s10661-009-0842-8>

Mertens, F.M., Pätzold, S., Welp, G., 2008. Spatial heterogeneity of soil properties and its mapping with apparent electrical conductivity. *J. Plant Nutr. Soil Sci.* 171, 146-154. <https://doi.org/10.1002/jpln.200625130> 2008

Moraes, M.C.P.D., Mello, K.D., Toppa, R.H., 2017. Protected areas and agricultural expansion: Biodiversity conservation versus economic growth in the Southeast of Brazil. *J. Environ. Manage.* 188, 73-84. <https://doi.org/10.1016/j.jenvman.2016.11.075>

Moral, F.J., Terrón, J.M., Marques da Silva, J.R.M., 2010. Delineation of management zones using mobile measurements of soil apparent electrical conductivity and multivariate geostatistical techniques. *Soil Till. Res.* 106, 335-343. <https://doi.org/10.1016/j.still.2009.12.002>

Nainggolan, D., de Vente, J., Boix-Fayos, C., Termansen, M., Hubacek, K., Reed, M.S., 2012. Afforestation, agricultural abandonment and intensification: Competing trajectories in semi-arid Mediterranean agro-ecosystems. *Agr. Ecosyst. Environ.* 159, 90-104. <https://doi.org/10.1016/j.agee.2012.06.023>

Noori, O., Panda, S.S., 2016. Site-specific management of common olive: Remote sensing, geospatial, and advanced image processing applications. *Comput. Electron. Agric.* 127, 680-689. <https://doi.org/10.1016/j.compag.2016.07.031>

Ortega-Blu, R., Molina-Roco, M., 2016. Evaluation of vegetation indices and apparent soil electrical conductivity for site-specific vineyard management in Chile. *Precis. Agric.* 17, 434-450. DOI 10.1007/s11119-016-9429-x

Öztekin, T., 2013. Short-term effects of land leveling on irrigation-related some soil properties in a clay loam soil. *Sci. World J.* 1-16. <https://doi.org/10.1155/2013/187490>

Panda, S.S., Hoogenboom, G., Paz, J.O., 2010. Remote sensing and geospatial technological applications for site-specific management of fruit and nut crops: a review. *Remote Sens.* 2, 1973-1997. <https://doi.org/10.3390/rs2081973>

Pedrerá-Parrilla, A., Van De Vijver, E., Van Meirvenne, M., Espejo-Pérez, A.J., Giráldez, J.V., Vanderlinden, K., 2016. Apparent electrical conductivity measurements in an olive orchard under wet and dry soil conditions:

POSTPRINT of the article: Uribeetxebarria, A., Daniele, E., Escolà, A., Arnó, J., Martínez-Casasnovas, J.A. 2018. Spatial variability in orchards after land transformation: Consequences for precision agriculture practices. *Sci. Total Environ.* 635, 343-352. <https://doi.org/10.1016/j.scitotenv.2018.04.153>

significance for clay and soil water content mapping. *Precis. Agric.* 17, 531-545. <https://doi.org/10.1007/s11119-016-9435-z>

Peralta, N.R., Costa, J.R., 2013. Delineation of management zones with soil apparent electrical conductivity to improve nutrient management. *Comput. Electron. Agric.* 99, 218-226. <https://doi.org/10.1016/j.compag.2013.09.014>

Peña-Barragán, J.M., Jurado-Expósito, M., López-Granados, F., Atenciano, S., Sánchez-de la Orden, M., García-Ferrer, A., García-Torres, L., 2004. Assessing land-use in olive groves from aerial photographs. *Agr. Ecosyst. Environ.* 103, 117-122. <https://doi.org/10.1016/j.agee.2003.10.014>

Priori, S., Martini, E., Andrenelli, M.C., Magini, S., Agnelli, A.E., Bucelli, P., Biagi, M., Pellegrini, S., Costantini, E.A.C., 2013. Improving Wine Quality through Harvest Zoning and Combined Use of Remote and Soil Proximal Sensing. *Soil Sci. Soc. Am. J.* 77, 1338-1348. <https://doi.org/10.2136/sssaj2012.0376>

Ramos M.C., Martínez-Casasnovas, J.A., 2010. Effects of field reorganisation on the spatial variability of runoff and erosion rates in vineyards of Northeastern Spain. *Land Degrad. Dev.* 21, 1-12, <https://doi.org/10.1002/ldr.958>

Rhoades, J.D., Chanduvi, F., Lesch, S., 1999. Soil salinity assessment: methods and interpretation of electrical conductivity measurements. *FAO Irrigation and Drainage Paper 57*. FAO: Rome, Italy, 150 pp, ISSN 0254-5284

Richter, H.G., 1984. Land use and land transformation. *GeoJournal* 8, 67-74. <https://doi.org/10.1007/BF00155612>

Rouse, J.W. Jr, Haas, R.H., Deering, D.W., Schell, J.A., Harlan, J.C., 1974. Monitoring the Vernal Advancement and Retrogradation (GreenWave Effect) of Natural Vegetation, NASA/GSFC Type III Final Report: Greenbelt, MD, USA, 371p.

Stassen, P., Wooldridge, J., 2011. Peach rootstocks for soil with moderately high pH and salinity. *SA Fruit J.* 34-38.

Soil Survey Staff, 2014. Keys to Soil Taxonomy, 12th ed., United States Department of Agriculture: Washington DC, USA.

Su, S., Zhou, X., Wan, C., Li, Y., Kong, W., 2016. Land use changes to cash crop plantations: crop types, multilevel determinants and policy implications. *Land Use Policy* 50, 379-389. <https://doi.org/10.1016/j.landusepol.2015.10.003>

Sudduth, K.A., Kitchen, N.R., Wiebold, W.J., Batchelor, W.D., Bollero, G.A., Bullock, D.G., Clay, D.E., Palm, H.L., Pierce, F.J., Schuler, T.T., Thelen, K.D., 2005. Relating apparent electrical conductivity to soil properties across the north-central USA. *Comput. Electron. Agric.* 46, 263-283. <https://doi.org/10.1016/j.compag.2004.11.010>

Tanji, K.K., Kielen, N.C., 2002. Agricultural drainage water management in arid and semi-arid areas. *FAO Irrigation and Drainage paper 61*. FAO: Rome, Italy, 188 pp, ISSN 0254-5284.

Taylor, J.A., McBratney, A.B., Whelan, B.M., 2007. Establishing management classes for broadacre grain production. *Agron. J.* 99, 1366-1376. <https://doi.org/10.2134/agronj2007.0070>

Uribeetxebarria, A., Arnó, J., Escolà, A., Martínez-Casasnovas, J.A., 2018. Apparent electrical conductivity and multivariate analysis of soil properties to assess soil constraints in orchards affected by previous parcelling. *Geoderma* 319, 185-193. <https://doi.org/10.1016/j.geoderma.2018.01.008>

POSTPRINT of the article: Uribeetxebarria, A., Daniele, E., Escolà, A., Arnó, J., Martínez-Casasnovas, J.A. 2018. Spatial variability in orchards after land transformation: Consequences for precision agriculture practices. *Sci. Total Environ.* 635, 343-352. <https://doi.org/10.1016/j.scitotenv.2018.04.153>

Wallace, J.F., Canci, M., Wu, X., Baddeley, A., 2008 Monitoring native vegetation on an urban groundwater supply mound using Airborne Digital Imagery. *J. Spat. Sci.* 53, 63–73. <http://dx.doi.org/10.1080/14498596.2008.9635136>

Xiao, R., Su, S., Mai, G., Zhang, Z., Yang, C., 2015. Quantifying determinants of cash crop expansion and their relative effects using logistic regression modeling and variance partitioning. *Int. J. Appl. Earth Obs. Geoinf.* 34, 258-263. <https://doi.org/10.1016/j.jag.2014.08.015>

Ye, X., Sakai, K., Sasao, A., Asada, S., 2009. Estimation of citrus yield from canopy spectral features determined by airborne hyperspectral imagery. *Int. J. Remote Sens.* 30, 4621-4642. <https://doi.org/10.1080/01431160802632231>

Yi, Z., Cannon, C.H., Chen, J., Ye, C., Swetnam, R.D., 2014. Developing indicators of economic value and biodiversity loss for rubber plantations in Xishuangbanna, southwest China: a case study from Menglun township. *Ecol. Indic.* 36, 788–797. <https://doi.org/10.1016/j.ecolind.2013.03.016>

Zarco-Tejada, P.J., González-Dugo, M.V., Fereres, E., 2016. Seasonal stability of chlorophyll fluorescence quantified from airborne hyperspectral imagery as an indicator of net photosynthesis in the context of precision agriculture. *Remote Sens. Environ.* 179, 89–103. <https://doi.org/10.1016/j.rse.2016.03.024>

Zude-Sasse, M., Fountas, S., Gemtos, T.A., Abu-Khalaf, N., 2016. Applications of precision agriculture in horticultural crops. *Eur. J. Hortic. Sci.* 81, 78–90. <https://doi.org/10.17660/eJHS.2016/81.2.2>